JOURNAL OF BACTERIOLOGY, Mar. 2003, p. 1599–1607 Vol. 185, No. 5
0021-9193/03/$08.00+0 DOI: 10.1128/JB.185.5.1599–1607.2003

Multiple Light Inputs Control Phototaxis in *Synechocystis* sp. Strain PCC6803†

Wing-On Ng,* Arthur R. Grossman, and Devaki Bhaya

Department of Plant Biology, Carnegie Institution of Washington, Stanford, California 94305

Received 29 August 2002/Accepted 3 December 2002

The phototactic behavior of individual cells of the cyanobacterium *Synechocystis* sp. strain PCC6803 was studied with a glass slide-based phototaxis assay. Data from fluence rate-response curves and action spectra suggested that there were at least two light input pathways regulating phototaxis. We observed that positive phototaxis in wild-type cells was a low fluence response, with peak spectral sensitivity at 645 and 704 nm. This red-light-induced phototaxis was inhibited or photoreversible by infrared light (760 nm). Previous work demonstrated that a *taxD1* mutant (Cyanobase accession no. sll0041; also called *pisJ1*) lacked positive but maintained negative phototaxis. Therefore, the TaxD1 protein, which has domains that are similar to sequences found in both bacteriophytochrome and the methyl-accepting chemoreceptor protein, is likely to be the photoreceptor that mediates positive phototaxis. Wild-type cells exhibited negative phototaxis under high-intensity broad-spectrum light. This phenomenon is predominantly blue light responsive, with a maximum sensitivity at approximately 470 nm. A weakly negative phototactic response was also observed in the spectral region between 600 and 700 nm. A Δ*taxD1* mutant, which exhibits negative phototaxis even under low-fluence light, has a similar action maximum in the blue region of the spectrum, with minor peaks from green to infrared (500 to 740 nm). These results suggest that while positive phototaxis is controlled by the red light photoreceptor TaxD1, negative phototaxis in *Synechocystis* sp. strain PCC6803 is mediated by one or more (as yet) unidentified blue light photoreceptors.

Phototactic responses may enable cyanobacteria to position themselves for optimal light capture and efficient photosynthesis and may also facilitate escape from harmful UV radiation (7). Phototaxis is therefore an important element of acclimatization that reduces the potential for light stress in cyanobacteria. Phototactic responses are not uniform over the spectrum of light but are more sensitive to specific light wavelengths. For example, positive phototactic movement in the filamentous cyanobacterium *Phormidium uncinatum* is most sensitive to light of 390, 480, and 560 nm (18). The positive phototactic response of another filamentous cyanobacterium, *Cylindrospermum alatosporum*, peaks at about 450 nm and 640 nm. Similar action maxima have been reported for the cyanobacterium *Anabaena variabilis* except that two additional peaks were observed at 550 and 730 nm (18).

Recently, the action spectrum for phototaxis was determined for the thermophilic unicellular cyanobacterium *Synechococcus elongatus* (22). Low-intensity (3 μmol m^{-2} s^{-1}) red light caused the most pronounced positive phototactic response, with a spectral peak at about 640 nm. As the light intensity was increased, sensitivity in the green (530 nm) and infrared (720 nm) regions of the spectrum was observed. Negative phototaxis in this organism was not observed even at the highest fluence rates used (30 to 90 μmol m^{-2} s^{-1}).

Specific cyanobacteria and purple photosynthetic bacteria have been reported to exhibit negative phototaxis. A recent report suggested that *Synechocystis* sp. strain PCC6803 exhibited weakly negative phototaxis in long-wavelength UV irradiation (360 nm) (8). In the filamentous cyanobacterium *Anabaena variabilis*, negative phototaxis was elicited by green light of 500 to 560 nm and red light at wavelengths above 700 nm (28). Differences in the spectral profiles that elicit phototactic responses among cyanobacteria may reflect the diverse light environments in which these organisms live. The photoreceptors associated with these responses may have evolved to accommodate the spectral features of specific environments.

Like many cyanobacteria, *Synechocystis* sp. strain PCC6803 exhibits robust phototaxis. One input sensor for this process appears to be the putative photoreceptor TaxD1 (Cyanobase accession no. sll0041; synonym, PisJ1), which has sequence similarity to both bacteriophytochromes and methyl-accepting chemoreceptor proteins (2, 39). In a model based on genetic evidence and knowledge of the chemotaxis paradigm, regulatory elements analogous to those that control bacterial chemotaxis are proposed to serve a major function in modulating the phototactic responses of *Synechocystis* sp. strain PCC6803 (2). The involvement of chemotaxis-like transducers (i.e., methyl-accepting chemoreceptor proteins and downstream signal transduction elements) in phototaxis was first described for haelobacteria (34). Specifically, light signals perceived by the putative photoreceptor TaxD1 are thought to trigger a phosphorylation cascade involving the histidine kinase TaxAY1, which in turn modulates the activity of the motility motor (3). Furthermore, other regulatory elements with homology to chemosensory proteins appear to be involved in the biogenesis of the motility apparatus itself (2).

The work reported in this article focuses on elucidating the intensity- and wavelength-dependent nature of phototactic responses of *Synechocystis* sp. strain PCC6803 and the role that

* Corresponding author. Present address: Civil and Environmental Engineering, Rm. B25, Terman Engineering Center, 380 Panama Mall, Stanford University, Stanford, CA 94305-4020. Phone: (650) 725-3025. Fax: (650) 725-2962. E-mail: wng@stanford.edu.

† This is Carnegie Institution DPB publication no. 1604.

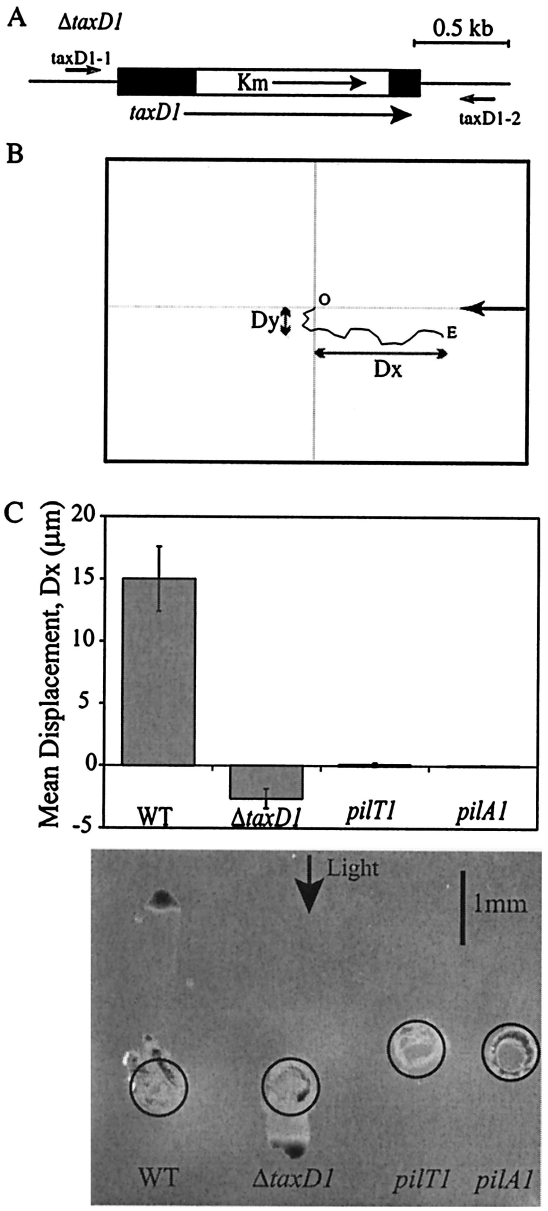

FIG. 1. (A) Construct used for generating Δ*taxD1* deletion mutant. Black rectangles represent the remaining coding region of *taxD1*. The kanamycin resistance cassette is represented by the open rectangle (indicated by Km). Black arrows indicate the direction of transcription. Relative locations of the primers taxD1-1 and taxD1-2 with respect to the *taxD1* gene are shown. (B) Analysis of phototactic movement with the glass slide-based assay. The cell track is indicated by the solid line. O, origin; E, end. *Dx*, displacement along the *x* axis; *Dy*, displacement along the *y* axis; arrow, direction of the incident light. (C) Comparison of the glass slide-based and agar surface-based phototaxis assays. Top panel, average displacement (*Dx*) of cells in unidirectional light with the glass-based phototaxis assay. Phototaxis in a population of *Synechocystis* sp. strain PCC6803 cells was recorded for 175 s and quantified. The light source was a low-noise illuminator, as in Fig. 1. Fluence rate was 19.3 μmol m^{-2} s^{-1}. Each bar represents the average of the mean displacement from three independent populations of the wild-type (WT), Δ*taxD1*, *pilT1*, and *pilA1* mutant cells. Error bars represent 1 standard deviation from the mean. Positive displacement = towards light; negative displacement = away from light. Bottom panel, average displacement (*Dx*) of cells in unidirectional light with the agar-based phototaxis assay. Cells were applied to the surface of 0.5% agar with a micropipette and placed in front of a unidirectional light source for 48 h. Circles indicate the original positions of applied cells. Arrow indicates the direction of light. The light source was a Philips Cool White fluorescent lamp (FT20T12/CW). Fluence rate was 5.3 μmol m^{-2} s^{-1}.

TaxD1 plays in controlling these responses. By comparing phototactic responses in wild-type and *taxD1* mutant cells, we dissected the spectral and fluence sensitivity of the photoreceptor(s) mediating both positive and negative phototaxis. These physiological measurements demonstrated that at least two photoreceptors with different fluences and spectral sensitivities are required for phototaxis in *Synechocystis* sp. strain PCC6803 and that at least one of these photoreceptors has photoreversible characteristics similar to those of phytochromes in vascular plants.

MATERIALS AND METHODS

Strains and culture conditions. A motile isolate of *Synechocystis* sp. strain PCC6803 (referred to as the wild type) and mutants were grown in BG-11 medium or BG-11 supplemented with 10 μg of kanamycin sulfate per ml for the *taxD1* deletion mutant (Δ*taxD1*) or 10 μg of chloramphenicol per ml for the *pilT1* and *pilA1* mutants (1). Solid medium was prepared by adding either 1% (wt/vol) Bacto agar to the BG-11 medium for normal subculturing of cells or 0.5% (wt/vol) Bacto agar to BG-11 medium for analyzing phototaxis on an agar surface. *Escherichia coli* strain Top 10 [F^- *mcrA* Δ(*mrr-hsdRMS-mcrBC*) ϕ80 *lacZ*Δ*M15* Δ*lacX74 deoR recA1 araD139* Δ(*ara-leu*)*7697 galU galK rpsL* (Str^r) *endA1 nupG*] (Invitrogen, Carlsbad, Calif.) was used for routine cloning of DNA. All reagents were from Sigma-Aldrich Co., St. Louis, Mo.

Deletion within *taxD1*. The *taxD1* gene was amplified from *Synechocystis* sp. strain PCC6803 genomic DNA by PCR with the primer pair taxD1-1 (5′-GAC CCTTGATGGCGCTCTTTTT-3′) and taxD1-2 (5′-CGCCCCGCCCTTAATG GAATG-3′) (see Fig. 1). The resulting 3.6-kbp PCR product was cloned into the pGEM-T Easy vector (Promega, Madison, Wis.) and then transformed into *E. coli* strain Top 10. The resulting plasmid, pNG23, was digested with *Bst*EII to excise a 2.1-kbp fragment from within the *taxD1* open reading frame, removing approximately 79% of the *taxD1* coding region. The *Bst*EII ends of the plasmid were filled in with T4 DNA polymerase (New England Biolabs, Beverly, Mass.) and ligated to the *Hin*cII-*Hin*cII fragment from p34S-Km (13), which contains a gene that confers kanamycin resistance to recipient cells. The resulting plasmid, pNG29, was transformed into *Synechocystis* sp. strain PCC6803 as previously described (26) to generate the deletion mutant Δ*taxD1*. Successful deletion of the *taxD1* gene was confirmed by PCR with the taxD1-1/taxD1-2 primer pair (data not shown).

Agar surface-based phototaxis assay. Wild-type and Δ*taxD1*, *pilA1*, and *pilT1* mutant cells were cultured on soft BG-11 agar (0.5% agar) for 2 days under continuous unilateral illumination from two Philips Cool White fluorescent lamps (FT20T12/CW) at a fluence rate of ≈5 μmol m^{-2} s^{-1}. Δ*taxD1* and wild-type cells at the migration front were collected and spotted onto solid BG-11 medium containing 0.5% agar. Cells were then exposed to a unidirectional light source, as described above, at a fluence rate of 5.3 μmol m^{-2} s^{-1} for 48 h.

Glass slide-based phototaxis assay. Wild-type and Δ*taxD1*, *pilA1*, and *pilT1* mutant cells were trained with a unidirectional light source as described above. Δ*taxD1* and wild-type cells at the migration front were collected and resuspended in 20 to 30 μl of fresh liquid BG-11 medium to a concentration of about 10^7 cells ml^{-1}. Then 6 μl of the cell suspension was immediately placed on a Fisherbrand Superfrost/Plus microscope slide (Fisher Scientific, Pittsburgh, Pa.). With the help of a micropipette tip, a coverslip (Esco Microscope cover glass, 18 by 18 mm, no. 1 thickness; Erie Scientific, Portsmouth, N.H.) was gently positioned over the cell suspension to avoid trapping air bubbles between the coverslip and slide. Excess liquid at the coverslip edges was carefully removed with a piece of tissue paper. To lessen evaporation from the sample, the edges of the coverslip were sealed with melted (70°C) Bioloid embedding paraffin (melting point, 56 to 58°C) (Will Corporation, New York, N.Y.). Alternatively, home canning wax (Walnut Hill Company, Bristol, Pa.) was used as a sealant. The slide with the assay chamber was placed on the microscope platform and illuminated with unfiltered condenser light (intensity of approximately 3 μmol m^{-2} s^{-1}). Cells were allowed to stabilize and settle onto the glass surface for 10 min. Assay

chambers that showed signs of mass liquid flow, inferred from a strong directional cell movement in the absence of lateral illumination, were discarded.

The unidirectional light source was provided by a Cole Parmer 9741-50 low-noise illuminator. Broad-spectrum output light (see the supplementary information at http://carnegiedpb.stanford.edu/research_bhaya.php, Fig. A1) from the halogen lamp of the illuminator was channeled through an optical fiber cable that was positioned in line with the long axis of the microscope slide. Illumination of the phototaxis assay chamber was done at an angle of 20° to the horizontal plane of the specimen platform. The profile of the light source was taken at 50% of maximum output. Fluence output was modulated by controlling the output dial of the illuminator or by using neutral density filters. The overall shape of the output profile did not change significantly at different output settings. The output fluence rate was measured with an LI-1800 portable spectroradiometer equipped with an 1800-11 Cosine remote receptor and calibrated with a 1800-02 optical radiation calibrator (LI-COR, Lincoln, Neb.).

Cell movement was viewed through a Nikon Eclipse TE300 inverted microscope with a 20× objective. Images were acquired with a CoolSnap-Pro digital camera and Image-Pro Express software (Media Cybernetics, Silver Spring, Md.). The microscope condenser light used for imaging cells was placed under the control of a shutter. To avoid interference by the condenser light with the movement of cells towards the lateral light source, the condenser light was filtered with a Balzer infrared interference filter with peak transmission at 840 nm (the fluence rate of the 840-nm light was not measured because it was beyond the range of the spectroradiometer). The shutter was set to an exposure time of 300 ms, and the time between exposures was 4.7 s, creating a 5-s interval between frames.

In experiments to validate the glass slide-based phototaxis assay (Fig. 1C, upper panel) and to establish the relationship between phototactic movement and fluence rates (Fig. 2), 36 frames were acquired for a total of 175 s for each movie. Three movies on three independent populations of cells were recorded for each of the strains and at each fluence rate tested. The same video imaging settings were used to examine the inhibitory effect of infrared light on phototaxis except in two of the treatments, where a 760-nm interference filter (half-bandwidth, 8 nm) was used in place of the 840-nm filter. For the action spectra, the number of frames per movie was reduced to 21, yielding a total movie time of 100 s. Again, for each fluence rate examined, the data were captured in three replica movies.

Motion tracking and data analysis. Movement of individual cells in the movies was tracked with Metamorph software (Universal Imaging Corporation, Downingtown, Pa.). Cells that were in direct contact with other cells and cells that exhibited no movement or moved outside the field of view over the course of the movie were not included in the analyses. All movies capturing cell movement were taken at the center of the assay chamber because those at the very edges tended to remain stationary, possibly because of heat damage caused by the melted wax used to seal the chamber. Generally, over 30 individual cells from each movie were tracked and analyzed. Data were collected and processed by Metamorph and exported as a Microsoft Excel file (Microsoft Corporation, Redmond, Wash.). Final figures were prepared in Adobe Illustrator (Adobe Systems, San Jose, Calif.).

In each movie, only the absolute displacement (not total distance traveled) in the direction of the incident light (*Dx*) was used (Fig. 1B). The only exception is the data presented in Fig. 2B, for which the average total distance was evaluated. Movement of all objects toward and away from the incident light was averaged to determine the mean displacement of the cell population. Positive displacement and negative displacement indicate net movement towards and away from the incident light, respectively. In most cases, the population average of lateral displacement perpendicular to the incident light (*Dy*) (Fig. 1B) was small (±3 μm), confined to a narrow range around 0 (data not shown). Therefore, *Dx* was used in place of the *R* value reported in a previous publication (8) as a measure for phototaxis. In the absence of unilateral light, the population average of *Dx* lies in a small range (±3 μm) around 0.

Action spectra. Three different action spectra were constructed for *Synechocystis* sp. strain PCC6803 and the Δ*taxD1*strain with a previously described method (29). The spectra were generated with illumination ranging from 394 to 740 nm. Balzers interference filters with half-band widths of 7 to 10 nm, as presented in the supplementary information at http://carnegiedpb.stanford.edu/research_bhaya.php, Table A1 (Unaxis USA Inc., Santa Clara, Calif.), were used to deliver narrow-bandwidth light. For many of the filters, the peak transmission is slightly shifted due mainly to the uneven spectral output from the light source (supplementary information at http://carnegiedpb.stanford.edu/research_bhaya.php, Fig. A1). Spacing between peak transmissions of the filters used for these studies ranged from 10 to 51 nm. The distribution of wavelengths used for generating the action spectra is not uniform and is concentrated in and around regions of the spectrum where phototaxis is maximum (to optimize the resolution of the action spectra).

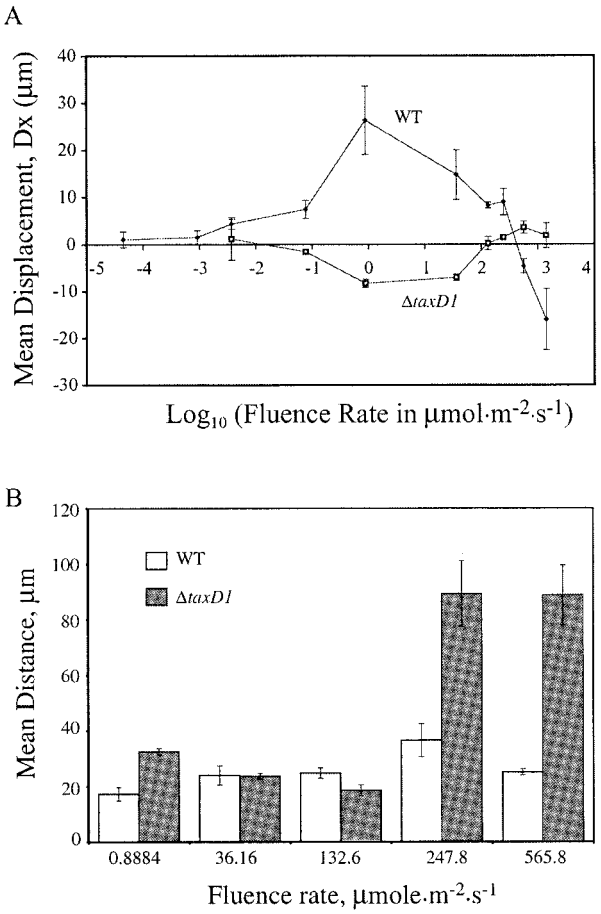

FIG. 2. (A) Average phototactic displacement (*Dx*) with respect to fluence rate in wild-type and Δ*taxD1* mutant cells of *Synechocystis* sp. strain PCC6803 in response to broad-spectrum light. Each point represents the average of the mean displacement from three independent populations of cells. Error bars represent 1 standard deviation from the mean. Positive displacement = towards light; negative displacement = away from light. (B) Mean total distance traveled by wild-type (WT, open bars) and Δ*taxD1* cells (shaded bars) at different fluence rates.

At each wavelength, different fluence rates were achieved by adjusting the illuminator output or by using neutral density filters. A fluence rate-response curve was constructed for each wavelength (see the supplementary information at http://carnegiedpb.stanford.edu/research_bhaya.php, Fig. A2 to A4). Each data point used to generate action spectra represents the population mean of *Dx* from three replicate movies. Data points in each plot were fitted to a straight line by linear regression analysis. In most cases, the coefficient of determination (R^2) was greater than 0.8, suggesting that the fluence rate response is near linearity.

To compile an action spectrum, the highest displacement recorded (*Dx*) among all wavelengths for each spectrum was set as the criterion response (29). For example, if the highest displacement recorded among all of the data generated for construction of an action spectrum is 60 μm, then the criterion response for the action spectrum is set at 60 μm. A fluence rate-response curve for a particular wavelength is extrapolated to the criterion response (Fig. 3A). The fluence rate at the criterion (*Fc*) is inversely proportional to the quantum efficiency of the wavelength. Therefore, the inverse of the fluence rate response at criterion (1/*Fc*) (expressed as a percentage of the highest response) is plotted against the wavelength to generate an action spectrum (Fig. 3B).

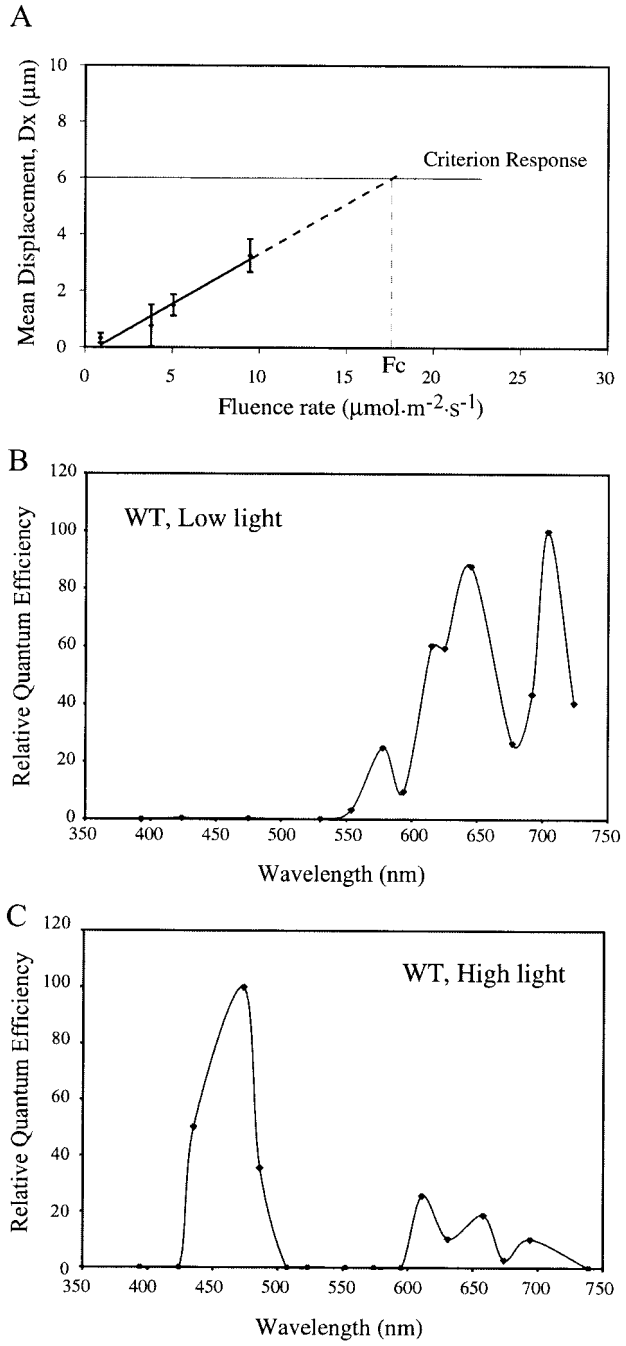

FIG. 3. (A) Method for calculation of quantum effectiveness of a particular wavelength of light in inducing phototaxis. Shown is a fluence rate-response curve for a particular wavelength. The fitted line is extrapolated to the criterion response. The fluence rate at the criterion response (*Fc*) is inversely proportional to the quantum effectiveness of the light used. Therefore, the inverse of *Fc* (1/*Fc*) is expressed as a percentage of the strongest response and then plotted against the wavelength to give the final action spectrum. (B) Action spectrum of positive phototaxis in wild-type (WT) *Synechocystis* sp. strain PCC6803 cells at low light intensity. (C) Action spectrum of negative phototaxis in wild-type *Synechocystis* sp. strain PCC6803 cells at high light intensity. At the wavelengths 394, 424, 523, 552, 574, and 595 nm, only positive phototaxis was observed at the highest possible fluence rates (maximum output from the illuminator) used, which were 16.29, 79.65, 422.1, 498.5, 304.9, and 1,046 μmol m^{-2} s^{-1}, respectively. Therefore, the negative phototactic responsiveness of cells at these wavelengths was considered to be 0.

RESULTS

Glass slide-based phototaxis assay. Individual *Synechocystis* sp. strain PCC6803 cells attached to and moved along a glass surface. When the cells were exposed to a unidirectional light source, they showed strong positive phototactic movement. A similar observation was reported earlier (8), although we found that the quartz assay chamber used in the previous report yielded unsatisfactory results. Without tightly sealing the edges of the assay chamber, evaporation of the sample led to mass flow of liquid within the chamber, obscuring the actual migration pattern of cells. Therefore, we adopted the glass slide-based phototaxis assay with the following modifications: (i) the assay chamber was constructed from a microscope slide and coverslip and the *Synechocystis* sp. strain PCC6803 cell suspension was placed between the upper slide and lower coverslip surfaces; (ii) evaporation was minimized by sealing the edges of the coverslip with embedding wax; and (iii) the total volume of the assay chamber was reduced to about 5 μl, with a depth of about 15 μm.

The glass slide-based assay was used to investigate the phototactic behavior of wild-type *Synechocystis* sp. strain PCC6803 and three mutant strains impaired for phototaxis, Δ*taxD1* (negative phototaxis), *pilT1* (nonmotile), and *pilA1* (nonmotile) (1, 2) (Fig. 1). Phototaxis assays were conducted with diluted cell suspensions in which the cells were not in direct contact with each other. The glass slide-based assay was compared with the traditional motility assay performed on a soft agar surface (Fig. 1C) (1). The glass slide-based assay accurately reproduced the phototactic phenotypes obtained for wild-type Δ*taxD1*, *pilT1*, and *pilA1* mutant cells with the agar surface-based assay. In addition, the relative rates of movement of the wild-type strain and the Δ*taxD1* mutant in the two different systems were similar (Fig. 1C). These results suggested that the gross features of motility observed with the two different assay systems are similar, although the absolute rates of movement and the paths taken to achieve the final displacement in the direction of the incident light (*Dx*) may be different.

Fluence rate response of wild-type and Δ*taxD1* strains. The glass slide-based phototaxis assay was used to study the fluence rate responses of wild-type and Δ*taxD1* mutant cells (Fig. 2A). Phototactic responses were measured over eight orders of magnitude of fluence rate with a broad-spectrum halogen light source (see the supplementary information at http://carnegiedpb.stanford.edu/research_bhaya.php, Fig. A1). Positive phototaxis could be reproducibly detected in wild-type cells down to 10^{-3} μmol m^{-2} s^{-1} (Fig. 2A). In contrast, for the onset of negative phototaxis, the Δ*taxD1* strain required a fluence rate that was more than 10-fold higher (>10^{-2} μmol m^{-2} s^{-1}). At higher fluence rates, positive phototaxis in wild-type cells increased, reaching a maximum at about 1 μmol m^{-2} s^{-1}. In order to get an accurate measure of the optimum light intensity for phototaxis, more data points would be required.

It is clear that an increase in the fluence rate to 36 μmol m^{-2} s^{-1} (or above) had a negative impact on positive phototaxis, leading to a decline in positive displacement. This reduction trend continued until no net phototactic displacement was detected at ≈475 μmol m^{-2} s^{-1} (designated the transition point) (28). At light intensities greater than the transition point, wild-type cells reversed the direction of phototaxis and

began to glide away from the incident light. The Δ*taxD1* mutant exhibited significant negative phototaxis at an intensity of approximately 1 μmol m^{-2} s^{-1} (Fig. 2A). As in wild-type cells, the response declined to some extent at a fluence rate of 36 μmol m^{-2} s^{-1}. The mean population displacement reached the transition point at ≈130 μmol m^{-2} s^{-1}. A further increase in light intensity led to a small reversal of direction to positive phototaxis. However, the magnitude of this positive phototaxis was small and within the margin of error of the average *Dx* of cells in the absence of phototaxis (±3 μm around 0). Therefore, the assignment of this positive phototaxis in Δ*taxD1* cells at high light intensity is tentative.

Figure 2B shows the average total distance traveled by wild-type and Δ*taxD1* cells before and after the transition points. Wild-type cells displayed little change in photokinesis except for a very slight positive photokinesis (increase in speed with increasing fluence rate) (18) at the light intensity tested just before the transition point (248 μmol m^{-2} s^{-1}). The Δ*taxD1* cells, on the other hand, displayed little change in photokinesis at light intensities below the transition point (130 μmol m^{-2} s^{-1}) but a strong positive photokinesis above the transition point. Since wild-type and Δ*taxD1* cells remained strongly motile at all intensities examined, the low *x* displacement (*Dx*) that occurred around the transition point must be a consequence of reorientation of cells (a more randomized movement) and not due to changes in the rates of movement.

The fluence rate-response curves of wild-type and Δ*taxD1* cells revealed important aspects of phototaxis. Deletion of the *taxD1* gene, which encodes the putative photoreceptor involved in positive phototaxis, led to a number of changes in the tactic responses of *Synechocystis* sp. strain PCC6803. Δ*taxD1* cells no longer exhibited positive phototaxis and instead displayed negative phototaxis in low-intensity light. There was also a two- to threefold reduction in the degree of phototactic displacement in the mutant (relative to wild-type cells) at light intensities at which movement was most pronounced for both strains. In addition, the mutant exhibited an increase in the fluence threshold for phototaxis at low light and a decrease in the transition point fluence at high light.

Action spectra of wild-type cells. Action spectra were constructed from individual fluence rate-response curves at different wavelengths with the method of Quinones et al. (29). Individual fluence rate-response curves were fitted with a linear regression line as shown (Fig. 3A; also see the supplementary information at http://carnegiedpb.stanford.edu/research_bhaya.php, Fig. A2 to A4). Some of the regression lines have *x*-intercept value less than 0. This was attributed to the slight random fluctuation of average displacement in a population of cells. In the absence of any unidirectional light stimulation, *Synechocystis* sp. strain PCC6803 cells exhibited an average displacement in a narrow range around zero (±3 μm) (data not shown). Therefore, in the fluence rate-response curves, the region between ±3 μm around 0 represents the true baseline for zero phototactic response. This slight deviation in the average displacement represents about 10% of the maximal response and did not significantly alter the shape of the final action spectra.

At low fluence rates (<1 μmol m^{-2} s^{-1}), positive phototaxis was mainly elicited by red and far-red light (Fig. 3B). There were two prominent peaks, one at ≈645 nm and the other at ≈704 nm, and the magnitudes of these peaks were nearly identical. The phototactic response at 704 nm is not typically observed in other organisms. To eliminate the possibility that it was an artifact (due to the heat from the 704-nm light), we examined the phototactic responses of wild-type cells with the agar surface-based assay (see the supplementary information at http://carnegiedpb.stanford.edu/research_bhaya.php, Fig. A5). The agar surface-based assay confirmed that both wild-type cells and the Δ*taxD1* mutant responded to 704-nm light. This far-red peak is distinctly absent in the absorption spectra of purified bacteriophytochromes (16, 23). We also observed a prominent shoulder for positive phototaxis at about 610 nm, while little response occurred at wavelengths below 550 nm. The response maximum in the red region of the spectrum parallels the absorption characteristics of the red-light-absorbing form (Pr) of bacteriophytochrome (peak absorption, ≈660 nm; shoulder, ≈600 to 610 nm) (16, 23) and plant phytochromes (35).

The negative phototaxis response of wild-type cells in high light showed very different spectral sensitivity than the positive phototaxis response (Fig. 3C). Negative phototaxis is predominantly a blue-light response, with peak sensitivity at around 470 nm. Relatively minor peaks were observed in the red region of the spectrum (600 to 700 nm).

Photoreversal of positive phototaxis by infrared light. A major characteristic of phytochrome-mediated responses is the photoreversibility of the red-light-triggered response with far-red light (35). To test whether positive phototaxis in wild-type cells displayed a similar photoreversibility, we examined phototaxis in cells exposed to lateral red light (645 nm) in the presence of perpendicular illumination with a narrow wave band of light at 760 nm. The 760-nm light was chosen because it is in the region of the far-red spectrum adjacent to the peak of the action spectrum at 704 nm (Fig. 3B). Unlike red light (emission maximum at 645 nm) (Fig. 4, treatment 3), infrared light at 760 nm elicited a very weak stimulation of positive phototaxis in wild-type cells (Fig. 4, treatment 2). However, the 760-nm light had a strong antagonistic effect on positive phototaxis when applied perpendicular to the direction of phototactic movement (Fig. 4, treatments 4 and 5). A red-infrared light ratio of about 1:1 reduced the phototactic displacement by about 60% (Fig. 4, treatment 4). A 1:3 ratio of red to infrared light caused a 90% reduction in phototactic movement (Fig. 4, treatment 5).

Action spectrum of Δ*taxD1* cells. Unlike wild-type cells, the Δ*taxD1* mutant exhibited negative phototaxis even during exposure to low-fluence light. The action spectrum demonstrates that this phenomenon was predominantly responsive to blue light, with a maximum at 470 nm (Fig. 5), which resembles the action maximum for negative phototaxis in the wild-type cells. The similarity between the action spectrum for negative phototaxis in wild-type cells and the Δ*taxD1* mutant suggests that the photoreceptor(s) governing this response in the two strains is the same or closely related. However, unlike negative phototaxis in wild-type cells, the Δ*taxD1* strain responded to some extent to light in the spectral range from 500 to 600 nm. In addition, the Δ*taxD1* mutant exhibited a similar weakly negative phototactic response to red and infrared light (600 to 740 nm) (Fig. 5), as observed for wild-type cells (Fig. 3C). The major difference between negative phototaxis in wild-type cells

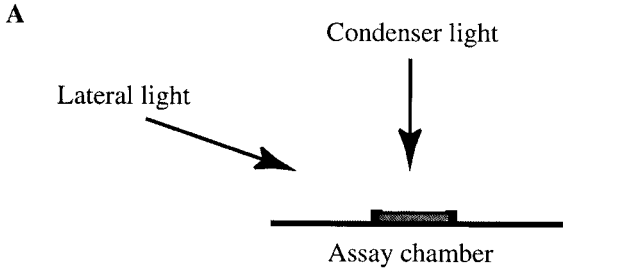

B

Treatments	1	2	3	4	5
Dark	+	-	-	-	-
Lateral-760 nm	-	+	-	-	-
Lateral-645 nm	-	-	+	+	+
Condenser-840 nm	+	+	+	-	-
Condenser-760 nm, A	-	-	-	+	-
Condenser-760 nm, B	-	-	-	-	+

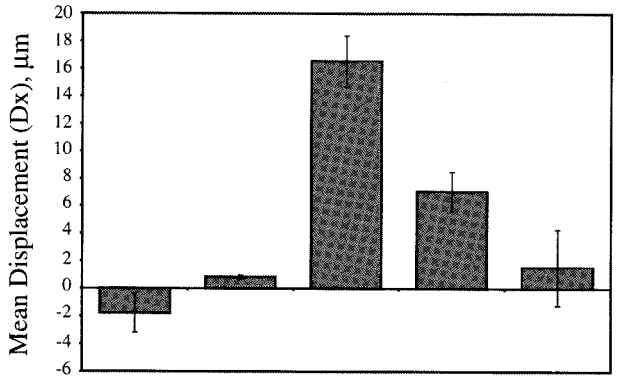

FIG. 4. Antagonistic effect of infrared light on positive phototaxis in wild-type cells. (A) Front view of the experimental setup, showing the assay chamber and directions of the condenser and lateral light. (B) Various light treatments are shown in the top table. The bar graph below the table shows the mean displacement of wild-type cells under the various light treatments. Each bar represents the average of the mean displacement from three independent populations of cells. Error bar represents 1 standard deviation from the mean. "Dark" indicates that no lateral illumination was used. The peak emissions for the lateral and condenser light sources are provided. Fluence rates used are as follows: Lateral, 760 nm, 0.6712 μmol m^{-2} s^{-1}; lateral, 645 nm, 0.5266 μmol m^{-2} s^{-1}; condenser, 760 nm: A, 0.4651 μmol m^{-2} s^{-1}; B, 1.552 μmol m^{-2} s^{-1}.

and the Δ*taxD1* mutant is that the fluence threshold for negative phototaxis is 1,000-fold higher for the former. These results suggest that TaxD1 either directly or indirectly influences the fluence dependency for negative phototaxis.

DISCUSSION

The glass slide-based assay for phototaxis has considerable advantages relative to the more traditional agar surface-based motility assay. The time necessary for generation and acquisition of data is extremely short (a few minutes), and the cell suspensions used can be relatively dilute, which makes it very easy to track individual cells. The short assay time of the glass slide-based assay also avoids the potential problem of nutrient deprivation within the assay chamber and makes it possible to evaluate phototactic responses at light levels inefficient at stimulating photosynthesis (long-term growth under such conditions could lead to metabolic difficulties). Furthermore, conducting the assays at low cell density avoids the potential problem of depletion of the incoming light of specific wavelengths as a consequence of self-screening of cells. However, it should also be kept in mind that the behavior of a single cell moving on a solid glass surface, bathed in liquid, is likely to be different from the coordinated movement of large populations of cells that straddle the interface between a hydrated agar surface and air. Previous work with *Myxococcus xanthus* has demonstrated that the movement of individual cells (adventurous motility) differed significantly from the movement of cells migrating as a large cell mass (social motility) (33).

Synechocystis sp. strain PCC6803 cells exhibited both positive and negative phototaxis in a fluence-dependent manner. Positive phototaxis was observed at fluence rates below the transition point of ≈475 μmol m^{-2} s^{-1}. As the light intensity increased beyond this point, cells responded by reversing the direction of taxis. Previous work has demonstrated that exposure of *Synechocystis* sp. strain PCC6803 cells to high-fluence light (≥500 μmol m^{-2} s^{-1}) causes rapid photoinhibition of photosynthesis (25). The comparable fluence rates for the transition point and the point at which photoinhibition begins suggest that the switch to negative phototaxis may represent a mechanism that helps protect *Synechocystis* sp. strain PCC6803 cells from the absorption of excessive excitation energy.

Two lines of evidence from earlier work suggested that TaxD1 is the photoreceptor critical for positive phototaxis. First, a *taxD1* mutant lacks positive phototaxis, and second, the TaxD1 polypeptide has domains similar to the light-sensing domain (chromophore-binding domain) of phytochromes of plants (and some bacteria) and the signaling domain of methyl-accepting chemoreceptors of bacteria (2, 39). In this report, we corroborate and extend these initial observations by showing that positive phototaxis in wild-type cells has a red-light-dominated action spectrum that is photoreversed by far-red light, consistent with the idea that positive phototaxis is controlled by a phytochrome-like photoreceptor. Furthermore, differences in the phototactic behavior of wild-type and Δ*taxD1* cells sug-

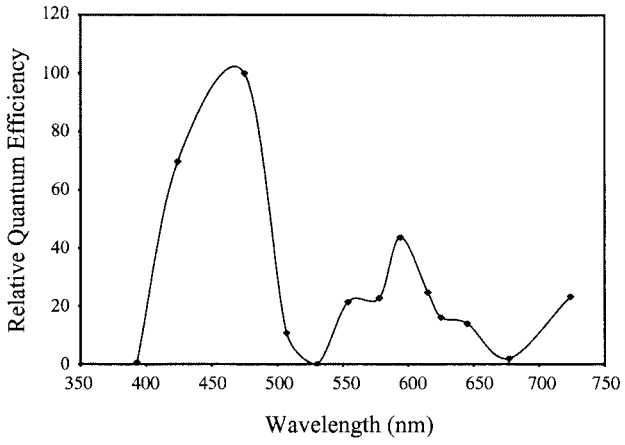

FIG. 5. Action spectrum of negative phototaxis in the Δ*taxD1* mutant of *Synechocystis* sp. strain PCC6803 cells at low light intensity.

TABLE 1. Phenotypic differences between wild-type and Δ*taxD1* cells

Strain	Phototactic response		Relative phototactic movement[a] (%)	Low-light phototaxis threshold (μmol m^{-2} s^{-1})	Fluence rate at transition point[b] (μmol m^{-2} s^{-1})	Spectral sensitivity[c]
	Low light	High light				
Wild type	Positive	Negative	100	$\sim 10^{-3}$	~475	Red-infrared (orange)
Δ*taxD1*	Negative	Positive	40	$\sim 10^{-2}$	~130	Blue (green-red)

[a] Net phototactic movement at 1 μmol m^{-2} s^{-1}.
[b] Reversal from positive to negative phototaxis in the wild type and from negative to positive phototaxis in the Δ*taxD1* mutant.
[c] Peak spectral regions that can induce phototaxis. Minor peaks are shown in parentheses.

gest that the TaxD1 protein is a low-fluence photoreceptor (Table 1). The threshold for the onset of positive phototaxis in wild-type *Synechocystis* sp. strain PCC6803 is comparable to the thresholds determined for phytochrome-mediated responses in vascular plants (20).

Bacterial phytochrome-like polypeptides have previously been associated with both responses to light quality and the biosynthesis of the photosynthetic apparatus (16, 17, 21), and in some cases they appear to be involved in establishing photoprotective processes (12, 36). Here we show a 645-nm action maximum for the positive phototaxis response, which is typical of action maxima for phytochrome-mediated responses in plants (35) and matches the in vitro absorption profile of purified phytochromes (16, 23, 35). Positive phototaxis in wild-type cells also displayed photoreversibility, another hallmark of phytochrome-mediated responses (35). Similar reversal of positive phototaxis has been reported for *S. elongatus* (22). Furthermore, red- and far-red-light photochromic shifts have been demonstrated for bacterial phytochromes synthesized in vitro and in vivo (5, 15, 32, 38), and recently a red-green light photochromic shift was demonstrated for the phytochrome-like protein involved in controlling complementary chromatic adaptation in the filamentous cyanobacterium *Fremyella diplosiphon* (D. Kehoe, personal communication).

Although the action spectrum for positive phototaxis in wild-type cells is similar to the absorption spectrum of phytochromes, it lacks the blue/UV-A peak typical of most phytochromes, and the prominent peak at around 704 nm in the action spectrum is more closely aligned with the far-red-light-absorbing form of phytochrome. These unusual features of the action spectrum suggest that the putative photoreceptor, TaxD1, may be an atypical phytochrome or that the features and activity of this putative phytochrome-like photoreceptor are modified by its associations in vivo. The existence of a second photoreceptor involved in modulating negative phototaxis was proposed based on studies of mutations in the *taxD1* gene (2). The Δ*taxD1* mutant is still phototactic but exhibits an inverted phototactic response under low-intensity illumination (Fig. 1 and 2). Wild-type cells also exhibited negative phototaxis but only upon exposure to high-intensity light (Fig. 2A). Action spectra for the negative phototactic responses in wild-type cells and the Δ*taxD1* mutant were similar, with a prominent peak in the blue region of the spectrum and other minor peaks at longer wavelengths (Fig. 3C and 5). From the available data, we conclude that a blue-light photoreceptor(s) with a spectral sensitivity that peaks at approximately 470 nm mediates negative phototaxis in *Synechocystis* sp. strain PCC6803. Our data cannot resolve the issue of whether a single photoreceptor mediates this response in both the wild-type and Δ*taxD1* mutant cells.

We do not know the exact nature of the photoreceptor(s) that mediates negative phototaxis. If this photoreceptor represents a single species, its spectral features, based on action maxima, appear to be distinct from those of other blue-light receptors, including cryptochromes (6, 24), phototropins (9, 10, 19), photoactive yellow protein (14), and sensory rhodopsins (34). The reduced form of cytochrome *c* exhibits a blue absorption maximum at ≈420 nm, with minor peaks between 500 to 600 nm. However, the blue absorption peak of cytochrome *c* is blue shifted by ≈50 nm relative to the peak for negative phototaxis, and so the absorption properties of cytochrome *c* do not ideally match the action spectra for negative phototaxis. While there is no ideal fit for the blue-light photoreceptor that controls negative phototaxis in *Synechocystis* sp. strain PCC6803, it must be kept in mind that a number of the photoreceptors discussed above could have significantly altered spectral properties when localized to specific cellular environments (associated with other proteins and/or integrated into membranes). Genetic identification of the blue-light photoreceptor(s) and the phenotype of strains compromised for its function will lead to a better understanding of the nature and number of photoreceptors involved in negative phototaxis.

There are a number of ways in which the phototactic responses of *Synechocystis* sp. strain PCC6803 may be controlled. Under low-light conditions, the signal from TaxD1 may actively suppress negative phototaxis. This suppression would be overcome at higher light intensities. Alternatively, in high-intensity light, the photoreceptor for negative phototaxis may be activated and suppress TaxD1 signaling. A third possibility is that there is a competition between light input signals that differentially affect the direction of motility by modulating the function of the motor apparatus; the final outcome of positive or negative phototaxis would depend simply on the relative strengths of the signals from the opposing input pathways.

The switch from positive to negative phototaxis at high light intensity in wild-type *Synechocystis* sp. strain PCC6803 cells was accompanied by a drastic spectral shift in the action spectra. This likely indicates a dose-dependent switch in the use of specific photoreceptors; as the light intensity is increased, phototactic responses elicited from a blue-light photoreceptor become dominant over those elicited from a red-light photoreceptor (TaxD1). The reversal of tactic responses in a dose-dependent fashion resembles reversal responses observed for several other tactic systems, such as those involved in aerotaxis and thermotaxis. Aerotaxis in *E. coli* is mediated through the Aer redox sensor and the serine chemoreceptor, Tsr (30). Cells

are attracted to low oxygen concentrations (≤0.25 mM) and repelled from higher oxygen concentrations (31). Mutational analysis of the CheB methylesterase has suggested that methylation of the chemoreceptor at high oxygen concentrations was responsible for reversal of the positive aerotaxis response (11).

The *E. coli* thermosensor Tar has been shown to be regulated by its methylation state in a similar manner (unmethylated = warm sensor; methylated = cold sensor) (27). This raises the intriguing possibility that the activity of TaxD1 can be regulated by a similar posttranslation modification. Based on sequence alignments, TaxD1 has two of the five conserved methylation sites present in Tar and Tsr (39). However, the *Synechocystis* sp. strain PCC6803 genome lacks the methyltransferase gene ortholog, *cheR* (39) (the CheR protein methylates the chemoreceptors). This lack of nucleotide sequence similarity, however, does not preclude the existence of a functional ortholog for *cheR* on the *Synechocystis* sp. strain PCC6803 genome.

Results presented here suggest that there are at least two functionally and spectrally distinct photoreceptors governing phototaxis in *Synechocystis* sp. strain PCC6803. Although the gene coding the putative positive phototaxis photoreceptor *taxD1* is known, the biochemical characteristics of the TaxD1 protein remain to be examined. A close match between the absorption spectrum of purified TaxD1 and the action spectrum for positive phototaxis would confirm a central role for this molecule as the photoreceptor that governs phototaxis. Furthermore, identification of the blue-light-responsive photoreceptor for negative phototaxis is crucial for understanding the transition from a positive to a negative phototactic response. However, some recent results suggest that there are additional interactions between blue- and red-light photoreceptors that might modulate phototactic responses. Wilde et al. (37) have recently shown that while low-intensity blue light did not induce motility in wild-type cells, a mutant deleted for *cph2* (encoding a phytochrome like polypeptide) moved towards blue light; the phytochrome-like Cph2 may be involved in inhibiting movement of wild-type cells towards blue light.

Characterization of numerous additional factors (3, 4) critical for normal phototaxis that may function downstream of the light signals will help establish the signal transduction pathway that communicates with motor function in *Synechocystis* sp. strain PCC6803 as well as the components required for the synthesis and maintenance of an active motor. Furthermore, it is clear that both the direction and magnitude of the phototactic responses involve multiple input pathways that are responsive to incident light intensity and quality.

ACKNOWLEDGMENTS

We thank Roberto A. Bogomolni, Winslow R. Briggs, and John M. Christie for helpful suggestions. We are also grateful to Winslow R. Briggs, Martin Lohr, and Trevor E. Swartz for comments on the manuscript.

This work was supported by the NSF (grant MCB 0110544 to D.B. and grant MCB 9727836 to A.G.) and by the Carnegie Institution of Washington.

REFERENCES

1. **Bhaya, D., N. R. Bianco, D. Bryant, and A. Grossman.** 2000. Type IV pilus biogenesis and motility in the cyanobacterium *Synechocystis* sp. PCC6803. Mol. Microbiol **37:**941–951.
2. **Bhaya, D., A. Takahashi, and A. R. Grossman.** 2001. Light regulation of type IV pilus-dependent motility by chemosensor-like elements in *Synechocystis* sp. strain PCC6803. Proc. Natl. Acad. Sci. USA **98:**7540–7545.
3. **Bhaya, D., A. Takahashi, P. Shahi, and A. R. Grossman.** 2001. Novel motility mutants of *Synechocystis* sp. strain PCC 6803 generated by in vitro transposon mutagenesis. J. Bacteriol. **183:**6140–6143.
4. **Bhaya, D., N. Watanabe, T. Ogawa, and A. R. Grossman.** 1999. The role of an alternative sigma factor in motility and pilus formation in the cyanobacterium *Synechocystis* sp. strain PCC6803. Proc. Natl. Acad. Sci. USA **96:** 3188–3193.
5. **Bhoo, S. H., S. J. Davis, J. Walker, B. Karniol, and R. D. Vierstra.** 2001. Bacteriophytochromes are photochromic histidine kinases with a biliverdin chromophore. Nature **414:**776–779.
6. **Cashmore, A. R., J. A. Jarillo, Y. J. Wu, and D. Liu.** 1999. Cryptochromes: blue light receptors for plants and animals. Science **284:**760–765.
7. **Castenholz, R. W., and F. Garcia-Pichel.** 2000. Cyanobacterial responses to UV-radiation, p. 591–611. *In* B. A. Whitton and M. Potts (ed.), The ecology of cyanobacteria. Kluwer Academic Publishers, Boston, Mass.
8. **Choi, J. S., Y. H. Chung, Y. J. Moon, C. Kim, M. Watanabe, P. S. Song, C. O. Joe, L. Bogorad, and Y. M. Park.** 1999. Photomovement of the gliding cyanobacterium *Synechocystis* sp. PCC 6803. Photochem. Photobiol. **70:**95–102.
9. **Christie, J. M., P. Reymond, G. K. Powell, P. Bernasconi, A. A. Raibekas, E. Liscum, and W. R. Briggs.** 1998. *Arabidopsis* NPH1: a flavoprotein with the properties of a photoreceptor for phototropism. Science **282:**1698–1701.
10. **Christie, J. M., M. Salomon, K. Nozue, M. Wada, and W. R. Briggs.** 1999. LOV (light, oxygen, or voltage) domains of the blue-light photoreceptor phototropin (*nph1*): binding sites for the chromophore flavin mononucleotide. Proc. Natl. Acad. Sci. USA **96:**8779–8783.
11. **Dang, C. V., M. Niwano, J. Ryu, and B. L. Taylor.** 1986. Inversion of aerotactic response in *Escherichia coli* deficient in CheB protein methylesterase. J. Bacteriol. **166:**275–280.
12. **Davis, S. J., A. V. Vener, and R. D. Vierstra.** 1999. Bacteriophytochromes: phytochrome-like photoreceptors from nonphotosynthetic eubacteria. Science **286:**2517–2520.
13. **Dennis, J. J., and G. J. Zylstra.** 1998. Improved antibiotic-resistance cassettes through restriction site elimination with Pfu DNA polymerase PCR. BioTechniques **25:**772–776.
14. **Devanathan, S., U. K. Genick, I. L. Canestrelli, T. E. Meyer, M. A. Cusanovich, E. D. Getzoff, and G. Tollin.** 1998. New insights into the photocycle of *Ectothiorhodospira halophila* photoactive yellow protein: photorecovery of the long-lived photobleached intermediate in the Met100Ala mutant. Biochemistry **37:**11563–11568.
15. **Foerstendorf, H., T. Lamparter, J. Hughes, W. Gartner, and F. Siebert.** 2000. The photoreactions of recombinant phytochrome from the cyanobacterium *Synechocystis*: a low-temperature UV-VIS and FT-IR spectroscopic study. Photochem. Photobiol. **71:**655–661.
16. **Giraud, E., J. Fardoux, N. Fourrier, L. Hannibal, B. Genty, P. Bouyer, B. Dreyfus, and A. Vermeglio.** 2002. Bacteriophytochrome controls photosystem synthesis in anoxygenic bacteria. Nature **417:**202–205.
17. **Grossman, A. R., D. Bhaya, and Q. He.** 2001. Tracking the light environment by cyanobacteria and the dynamic nature of light harvesting. J. Biol. Chem. **276:**11449–11452.
18. **Häder, D. P.** 1987. Photomovement, p. 325–345. *In* P. Fay and C. Van Baalen (ed.), The cyanobacteria. Elsevier, New York, N.Y.
19. **Huala, E., P. W. Oeller, E. Liscum, I. S. Han, E. Larsen, and W. R. Briggs.** 1997. *Arabidopsis* NPH1: a protein kinase with a putative redox-sensing domain. Science **278:**2120–2123.
20. **Kaufman, L. S., W. F. Thompson, and W. R. Briggs.** 1984. Different red light requirements for phytochrome-induced accumulation of *cab* RNA and *rbcS* RNA. Science **226:**1447–1449.
21. **Kehoe, D. M., and A. R. Grossman.** 1996. Similarity of a chromatic adaptation sensor to phytochrome and ethylene receptors. Science **273:**1409–1412.
22. **Kondou, Y., M. Nakazawa, S. Higashi, M. Watanabe, and K. Manabe.** 2001. Equal-quantum action spectra indicate fluence-rate-selective action of multiple photoreceptors for photomovement of the thermophilic cyanobacterium *Synechococcus elongatus*. Photochem. Photobiol. **73:**90–95.
23. **Lamparter, T., F. Mittmann, W. Gartner, T. Börner, E. Hartmann, and J. Hughes.** 1997. Characterization of recombinant phytochrome from the cyanobacterium *Synechocystis*. Proc. Natl. Acad. Sci. USA **94:**11792–11797.
24. **Lin, C., D. E. Robertson, M. Ahmad, A. A. Raibekas, M. S. Jorns, P. L. Dutton, and A. R. Cashmore.** 1995. Association of flavin adenine dinucleotide with the *Arabidopsis* blue light receptor CRY1. Science **269:**968–970.
25. **Mulo, P., S. Laakso, P. Mäenpää, and E. M. Aro.** 1998. Stepwise photoinhibition of photosystem II. Studies with *Synechocystis* species PCC 6803 mutants with a modified D-E loop of the reaction center polypeptide D1. Plant Physiol. **117:**483–490.
26. **Ng, W. O., and H. B. Pakrasi.** 2001. DNA photolyase homologs are the major UV resistance factors in the cyanobacterium *Synechocystis* sp. PCC 6803. Mol. Gen. Genet. **264:**924–930.
27. **Nishiyama, S., I. N. Maruyama, M. Homma, and I. Kawagishi.** 1999. Inversion of thermosensing property of the bacterial receptor Tar by mutations in the second transmembrane region. J. Mol. Biol. **286:**1275–1284.

28. **Nultsch, W., H. Schuchart, and F. Koenig.** 1983. Effects of sodium azide on phototaxis of the blue-green alga *Anabaena variabilis* and consequences to the two-photoreceptor systems-hypothesis. Arch. Microbiol. **134:**33–37.
29. **Quinones, M. A., Z. Lu, and E. Zeiger.** 1996. Close correspondence between the action spectra for the blue light responses of the guard cell and coleoptile chloroplasts, and the spectra for blue light-dependent stomatal opening and coleoptile phototropism. Proc. Natl. Acad. Sci. USA **93:**2224–2228.
30. **Rebbapragada, A., M. S. Johnson, G. P. Harding, A. J. Zuccarelli, H. M. Fletcher, I. B. Zhulin, and B. L. Taylor.** 1997. The Aer protein and the serine chemoreceptor Tsr independently sense intracellular energy levels and transduce oxygen, redox, and energy signals for *Escherichia coli* behavior. Proc. Natl. Acad. Sci. USA **94:**10541–10546.
31. **Shioi, J., C. V. Dang, and B. L. Taylor.** 1987. Oxygen as attractant and repellent in bacterial chemotaxis. J. Bacteriol. **169:**3118–3123.
32. **Sineshchekov, V., J. Hughes, E. Hartmann, and T. Lamparter.** 1998. Fluorescence and photochemistry of recombinant phytochrome from the cyanobacterium *Synechocystis*. Photochem. Photobiol. **67:**263–267.
33. **Spormann, A. M.** 1999. Gliding motility in bacteria: insights from studies of *Myxococcus xanthus*. Microbiol. Mol. Biol. Rev. **63:**621–641.
34. **Spudich, J. L.** 1998. Variations on a molecular switch: transport and sensory signalling by archaeal rhodopsins. Mol. Microbiol. **28:**1051–1058.
35. **Taiz, L., and E. Zeiger.** 1998. Phytochrome, p. 483–516. *In* Plant physiology. Sinauer Associates, Sunderland, Mass.
36. **Wilde, A., Y. Churin, H. Schubert, and T. Börner.** 1997. Disruption of a *Synechocystis* sp. PCC 6803 gene with partial similarity to phytochrome genes alters growth under changing light qualities. FEBS Lett. **406:**89–92.
37. **Wilde, A., B. Fiedler, and T. Börner.** 2002. The cyanobacterial phytochrome Cph2 inhibits phototaxis towards blue light. Mol. Microbiol. **44:**981–988.
38. **Yeh, K. C., S. H. Wu, J. T. Murphy, and J. C. Lagarias.** 1997. A cyanobacterial phytochrome two-component light sensory system. Science **277:**1505–1508.
39. **Yoshihara, S., F. Suzuki, H. Fujita, X. X. Geng, and M. Ikeuchi.** 2000. Novel putative photoreceptor and regulatory genes required for the positive phototactic movement of the unicellular motile cyanobacterium *Synechocystis* sp. PCC 6803. Plant Cell Physiol. **41:**1299–1304.